The International Journal of Advanced Manufacturing Technology (2019) 102:2451–2463
https://doi.org/10.1007/s00170-018-03270-0

ORIGINAL ARTICLE

# Contribution in analyzing dimensional deviations in ellipsoidal steel heads during deep drawing

H. Soltani[1] · A. Amirat[2] · O. Boussaid[3]

Received: 18 October 2018 / Accepted: 27 December 2018 / Published online: 1 February 2019


**Abstract**
The present work is a contribution in analyzing dimensional deviations in ellipsoidal thin-layer steel heads used for high-pressure air brake reservoirs. The dimensional deviations are attributed to the thickness distribution during the drawing process with regard to input geometrical parameters such as punch and die diameter, and also die and punch fillet. The aim of the present work is therefore optimizing the input data in order to respect the initial geometrical requirement. Investigation has been carried out using FEM code Abaqus, on a case example produced by the Algerian truck company according to G.R.C E81-102 standard. FEM simulations followed the process of deep drawing and concerned the effect of the most influencing factors such as the die corner radius, the punch corner radius, and the blank radius. Dimensional deviations are analyzed in terms of variations of thinning along the true dish path and hence engineering models of the corresponding true strain in the straight zone, the knuckle zone, and the crown zone of the dish are proposed.

**Keywords** Deep drawing · Thinning · Ellipsoidal heads · Steel · Die · Punch · Abaqus

## 1 Introduction

Air high-pressure reservoirs such as those used for air brake systems [1, 2] in heavy vehicles to reduce wheel speed or to stop them are designed to store compressed air so it is available for instant use. They are mainly composed of three parts made of thin-layer steel and assembled together by welding. So, much attention is focused on the manufacturing process of the parts in order to avoid any dimensional deviations that do not much the intended technical specifications and could affect the productivity and the quality of the product. These deviations can be generated by induced errors in length, width, curvature, and specific machined entities. Therefore, there is a need to identifying the sources of these deviations in order to respect the allowable dimensional tolerance range. For instance, ellipsoidal heads are parts that require specific production process in order to respect the G.R.C E81-102 standard. They are obtained by stamping a flat sheet steel using deep drawing process which consists in pressing the sheet by means of a purpose-shaped punch through a die. The stamping process suggests that all produced shapes have uniform cross section, but in practice, thinning and thickening usually occur because of a large amount of plastic deformations [3–5]. Therefore, it is important to know how much dimensional discrepancy can be permitted in order to warrant the reliability of the air brake system [6, 7]. Recent literature review papers have been dedicated to the deep forming making evidence of the need of assessment of the behavior of produced part by means of deep drawing. Li et al. [8] have presented a detailed literature review on the current research of incremental sheet forming related to deformation mechanism, modeling techniques, forming force prediction, and process investigations. A specific attention has been given

✉ H. Soltani
hanen_sol28@hotmail.fr

A. Amirat
amirat_abd@yahoo.fr

O. Boussaid
oboussaid@yahoo.fr

[1] Mechanics of Materials and Plant Maintenance Research Laboratory (LR3MI), Faculty of Engineering Sciences, Badji Mokhtar University Annaba, Annaba, Algeria

[2] Research Laboratory of Advanced Technology in Mechanical Production, Faculty of Engineering Sciences, Badji Mokhtar University Annaba, Annaba, Algeria

[3] Research Laboratory of Industrial Risks, Control and Safety, Faculty of Engineering Sciences, Badji Mokhtar University Annaba, Annaba, Algeria

to geometric accuracy, surface finish, and forming efficiency. Their review paper could act as an inspiration and reference for the researchers. Takalkar et al. [9] have proposed a review paper on effect of thinning, wrinkling, and spring-back on deep drawing process. They have focused on advanced methods for predicting defects like thinning, wrinkling, and spring-back on deep drawing process which are mostly responsible for rejection of the component. They have suggested an appropriate technique in order to achieve uniform thickness variation in drawn cup.

Research investigation on the dimension deviation during deep drawing process has known great interest [10, 11, 12]. For instance, Choi et al. [4] have developed a systematic numerical tool to assess the thermal deformation during a stamping process of an outer automotive body part. They have analyzed the input conditions such as the punch pressure, holder pressure, and friction coefficient in order to precisely control the dimensions of stamped parts and thus minimizing the dimensional deviation from its target values. In addition, they have reported that dimensional deviation is also affected by temperature that is generated on the one hand by temperature change due to the friction and plastic deformation and on the other hand by seasonal difference in the ambient temperature. The developed numerical procedure has been validated by experimental results. Takalkar et al. [13] have studied the effect of geometrical parameters such as punch nose radius and die shoulder radius on the rate of thickness variation of a cup-shaped component under multistage deep drawing process. Explicit numerical analyses have been carried out using two-dimensional full models in order to illustrate the thinning and the most probable failing zones during the cup deep drawing process. Choubey et al. [5] have numerically analyzed the thickness distribution of conical and cylindrical cups without blank holder using a conical die design. The thickness distribution is correlated to die and punch geometry, half-cone angle, die and punch fillet, and the drawing load when the cups are produced by pushing in a single stroke of the punch on the flat circular blanks. They reported good agreement between finite element simulation results and the mathematical and experimental results. Zheng et al. [14] based on extensive FEM simulations have proposed an empirical equation to predict the maximum plastic deformation during stamping of ellipsoidal heads of thin-walled pressure vessels to overcome no satisfactory solutions in predicting plastic deformation provided by current industrial standards. They have proposed equivalent plastic deformation (PEEQ) as a convenient parameter to characterize the deformation of the head stamping.

The present work is a contribution in analyzing dimensional deviations in ellipsoidal thin-layer steel heads during deep drawing process. As experimental investigation of the stamping process of ellipsoidal heads is difficult because of cost-related issues such as limited access to the process and high tooling costs, detailed analyses are approached by numerical simulation using the Abaqus code. The dimensional deviations are attributed to the thickness distribution during the drawing process with regard to input geometrical parameters such as punch and die radii, and also the fillet radius of the die and the punch. The aim of the present work is therefore optimizing the deep drawing input parameters in order to respect the initial geometrical requirement of a standard part. The case study concerns ellipsoidal heads of air high-pressure reservoirs used in air brake systems for heavy vehicles.

**Table 1** Chemical composition of DC04 steel in weight %

| Elements | *C* | *P* | *S* | Mn | Si |
|---|---|---|---|---|---|
| EN 10130 standard (%) | < 0.08 | < 0.03 | < 0.03 | < 0.4 | 0.08–0.1 |
| Diffractometry results (%) | 0.04 | 0.03 | 0.0033 | 0.4 | – |

## 2 Material, geometry, and process

### 2.1 Material

The material is a DC04 non-alloyed mild steel with high formability in all deformation modes used for deep drawing to produce automotive industrial parts. The chemical composition in weight % obtained by diffraction corresponded to that given by the standard EN10130 (Table 1). The mechanical properties (Table 2) and anisotropy behavior of the material are given in details in a recently published work by Ghennai et al. [15]. Meanwhile, tensile test on 2-mm-thick specimens is conducted to verify the behavior of the stress-strain curves throughout the three rolling directions (Fig. 1).

### 2.2 Geometry

The DC04 steel is used to produce ellipsoidal head parts for air pressure reservoirs of heavy vehicles' air brake systems as shown in Fig. 2.

### 2.3 Deep drawing process of the head part

The ellipsoidal head parts are manufactured in the Algerian trucks and buses factory SNVI Rouiba, in 12 operations. In the present work, attention is oriented to the deep drawing

**Table 2** Specific mechanical properties of DC04 for deep drawing

| Requirements | *E* (GPa) | $\sigma_{y0,2}$ (MPa) | $\sigma_{ts}$ (MPa) | A% |
|---|---|---|---|---|
| DC04 | 200–221 | 140–210 | 270–350 | 40 |

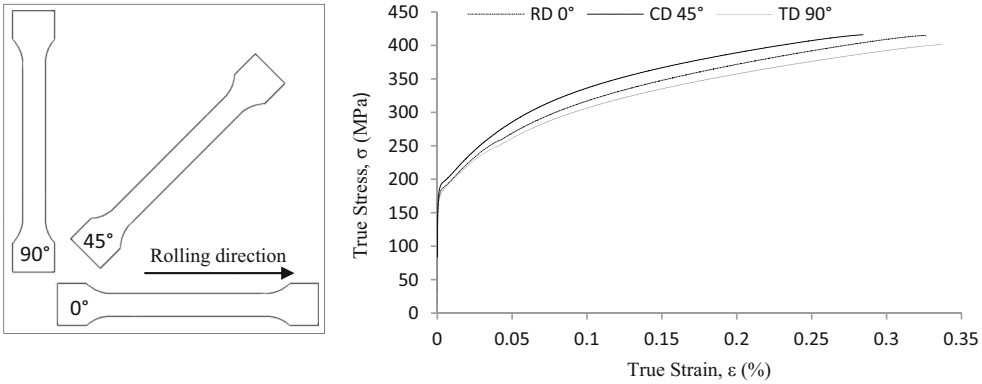


**Fig. 1** Effect of rolling direction on tensile properties

operation of the ellipsoidal head that is prepared according to G.R.C E81-102 standard. The deep drawing is carried out on a 300-T hydraulic drawing machine according to the schematic process illustration described in Fig. 3.

## 3 FEM simulations

There are two major issues to solve: first, respect the G.R.C E81-102 standard, and second, avoid any dangerous zone leading to shear of the drawn part. The most influencing factors on deep drawing of sheet metal are the die corner radius and the punch corner radius that generate a regular pressure distribution causing the metal to flow over the radius into the die cavity with minimum thinning of the initial thickness of the sheet metal and no defects. Meanwhile, the amount of clearance between the punch and the cavity of the die is also a factor that could cause cutting in the wall of the drawn part. These factors involve geometrical parameters that should be set in order to optimize the deep drawing process of the ellipsoidal head. Figure 4 illustrates the geometrical parameters to optimize when deep drawing an ellipsoidal head according to G.R.C E81-102 standard.

The FEM simulations are deduced from the deep process mechanism where the schematic illustration is given in Fig. 4. Figure 5 illustrates the process of the deep drawing and the corresponding maximum plastic elongation distribution while as the punch gets deeper. To achieve this task, FEM design simulations have been proposed as described in Table 3.

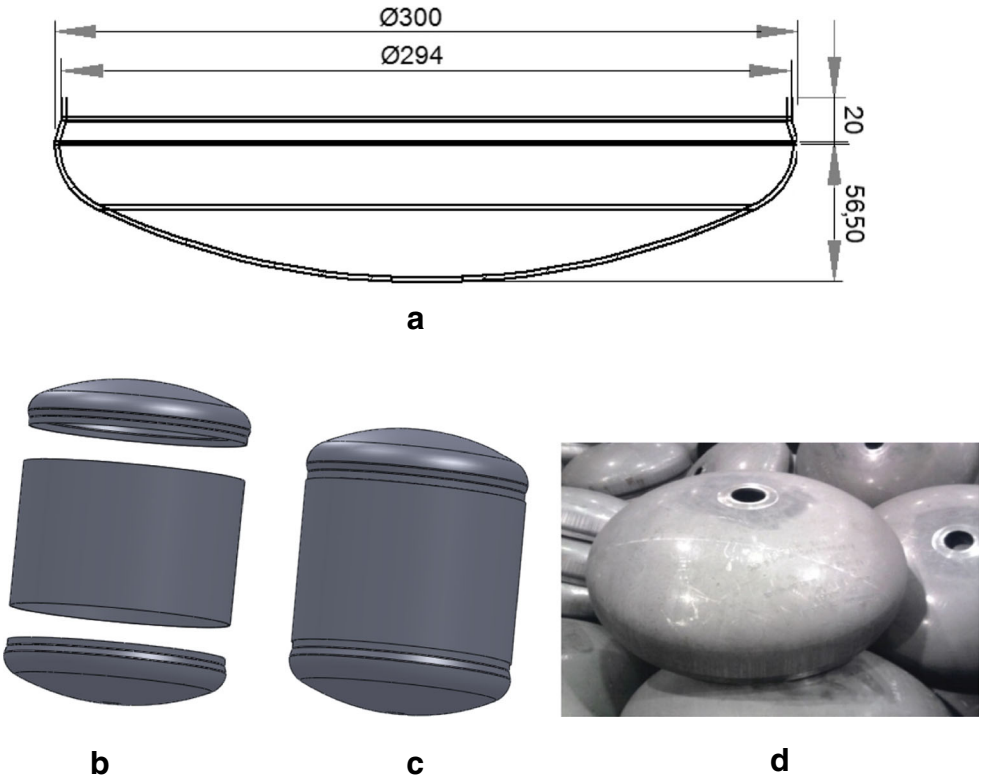


**Fig. 2** Geometry of air brake pressure reservoir head. **a** Geometry of the reservoir head. **b** Fitting parts of the reservoir. **c** Assembled reservoir by welding. **d** Head parts as manufactured

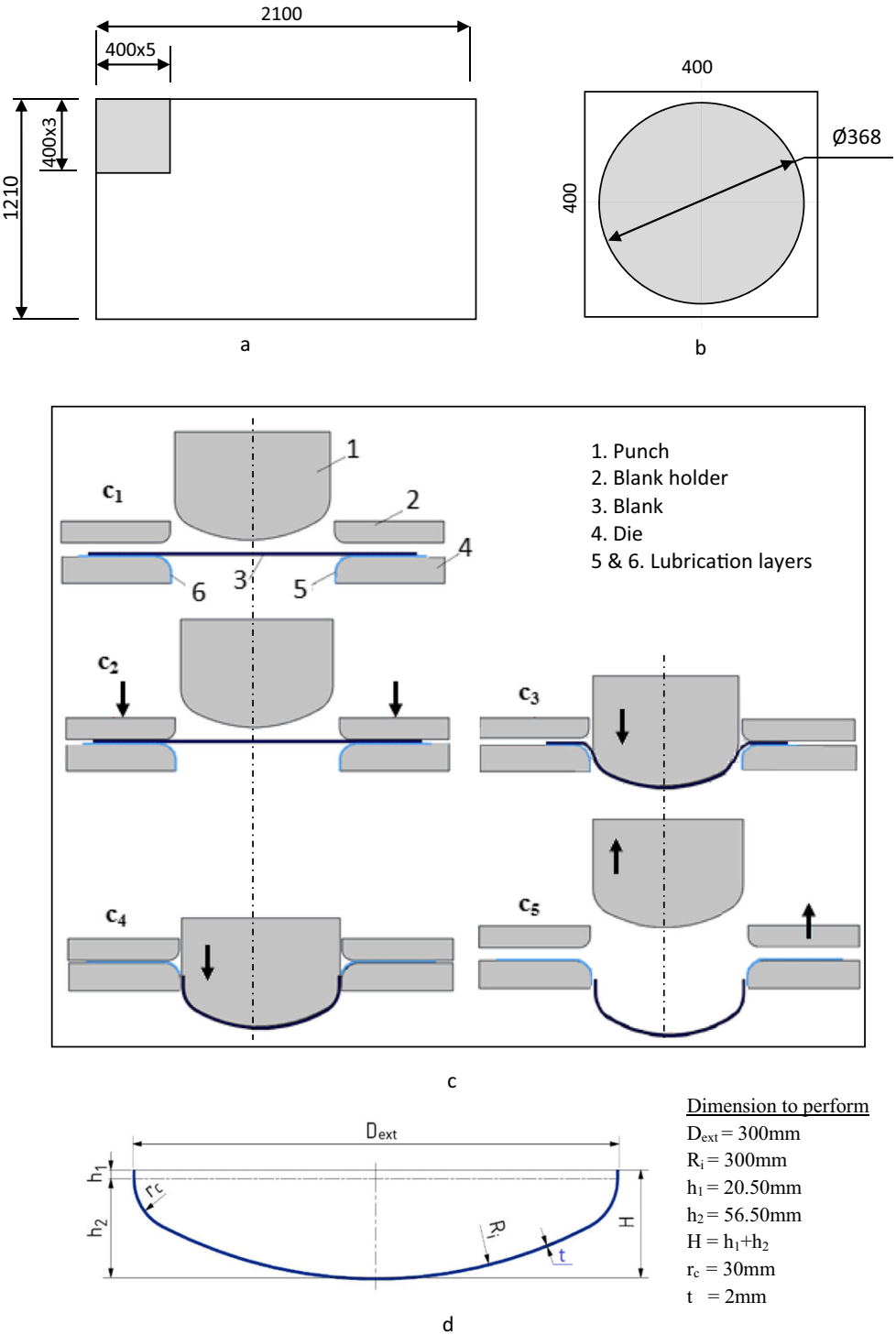


**Fig. 3** Schematic illustration of deep drawing of air brake pressure reservoir head. **a** Preparation of 15 square blanks from a parent steel sheet. **b** Press cutting of 368-mm-diameter blank. **c** Execution of the deep drawing process (the deep drawing process follows 5 main steps: step C1: setting blank on the die opening; step C2: clamping blank with sufficient force (1000 N) as to permit material flaw; step C3: making sure the punch is on the central line of the blank; step C4: pressing the punch downwards the blank through the cavity of the die until the head shape is obtained; step C5: removing up the punch and the shaped part). **d** Expected head part geometry

## 4 Optimizing input parameters in producing ellipsoidal head parts

### 4.1 Optimizing punch and die dimensions

The first approach of the present contribution consists in optimizing the head part geometry which must be fitted on the cylinder of the pressure reservoir then to be welded together. There are three (3) main parameters that should perform the geometry of the head part according to G.R.C E81-102 standard: the punch radius $p_r$, the bend radius of the punch $r_b$, and the die radius $D_r$. These three parameters are considered in the present work as performing geometry parameters. In industry, for a given external diameter of a head part to be produced, the

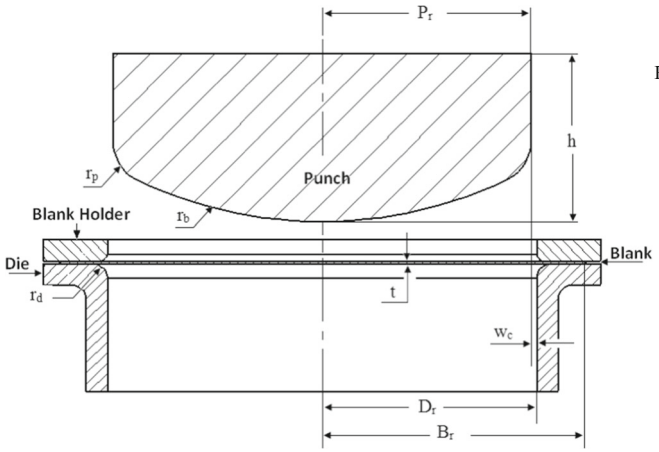


| Parameter | Designation |
|---|---|
| $B_r$ | Blank size radius |
| t | Blank thickness |
| $P_r$ | Punch radius |
| $r_p$ | Punch corner radius |
| $r_b$ | Bend radius |
| $D_r$ | Die radius |
| $r_d$ | Die corner radius |
| $w_c$ | Radial clearance between punch radius and die radius |
| h | Cup height of the first draw |

**Fig. 4** Geometrical parameters of the deep drawing system for drawing ellipsoidal heads of air brake pressure reservoirs

three performing geometry parameters are usually determined as a function of external diameter and set constant. The other parameters such as the punch corner radius, $r_p$, the die corner radius, $r_d$, and the radial clearance between punch radius and die radius, $W_c$, are used to regulate pressure distribution in order to let the metal flowing with minimum thinning of the initial thickness of the sheet metal and no defects. Therefore, the first approach is to check the industrial procedure through numerical analyses. In this case study, for an air pressure ellipsoidal head part (Fig. 3d) of 300-mm external diameter, the corresponding blank diameter is 368 mm.

#### 4.1.1 Effect of punch corner radius

The radius of the punch diameter may take different values that can affect the dimensional precision of the head part. So, the first five design simulations presented in Table 3 are attributed to the effect of punch corner radius variation from 26 to 34 mm. Meanwhile, the die corner is taken as used in industry with a value of 10 mm. Simulation results of the effect of variation of punch corner radius are given in Table 4.

When the punch corner radius increases, the overall dimensions of the ellipsoidal head are affected. Regarding the height of the dish, $H$ increases from 75.35 to 78.55 mm within a coefficient of variation of 0.19%. This results from the increases of $h_2$ from 54.87 to 58.20 while $h_1$ fluctuates around a mean value of 20.46 mm with a coefficient of variation of 0.17%. In the mean time, the external radius of the elliptical part of the head $R_i$ and the head corner radius of the dish $r_c$ increase as a function of the punch corner radius. The external diameter of the dish, $D_{ext}$, remains practically constant. The sensitivity to these geometrical parameters is expressed by their coefficient of variation (CV). Basically, the five design simulations agreed within very low coefficient of variation suggesting that the punch corner radius has little effect of the overall dimensions of the head part. However, the best performance is observed for the third design simulation which is in good agreement with the required values in industry. Therefore, the latter is adapted as a reference data for the coming numerical analyses.

#### 4.1.2 Effect of die corner radius

Relatively, the radius of the die corner may also take different values. So, the next five design simulations (6–10) are carried out with a punch corner radius of 30 mm, in order to determine the effect of the variation in the radius of the die corner on the dimensional quality of the head part, and results are summarized in Table 5.

When the die corner radius increases from 6 to 14 mm, the height of the dish, $H$, fluctuated around a value of 77.07 following the fluctuation of $h_1$ and $h_2$ around respectively 20.52 and 56.66 with a CV of 0.1%. The fluctuation of the latter values is observed in the radius of the elliptical part of the head $R_i$ that also fluctuated around 297.64 within a CV of 0.79%. The sensitivity of geometrical parameters is expressed by their CV. Basically, the low values of the coefficient of variation obtained for the five design experiments suggest that the die corner radius has little effect of the overall dimensions of the head part. However, the best performance is observed for the eighth design simulation which is in good agreement with the industrial application.

### 4.2 Optimizing blank diameter

The process of producing the ellipsoidal head according to the G.R.C E81-102 standard suggests that for a given external diameter, the diameter of the blank material should be determined as to avoid any thickening, thinning, or defects. Usually, the calculated blank diameter is readjusted on the site production until the standard dimensions are closely approached within the acceptable tolerances. However, it is

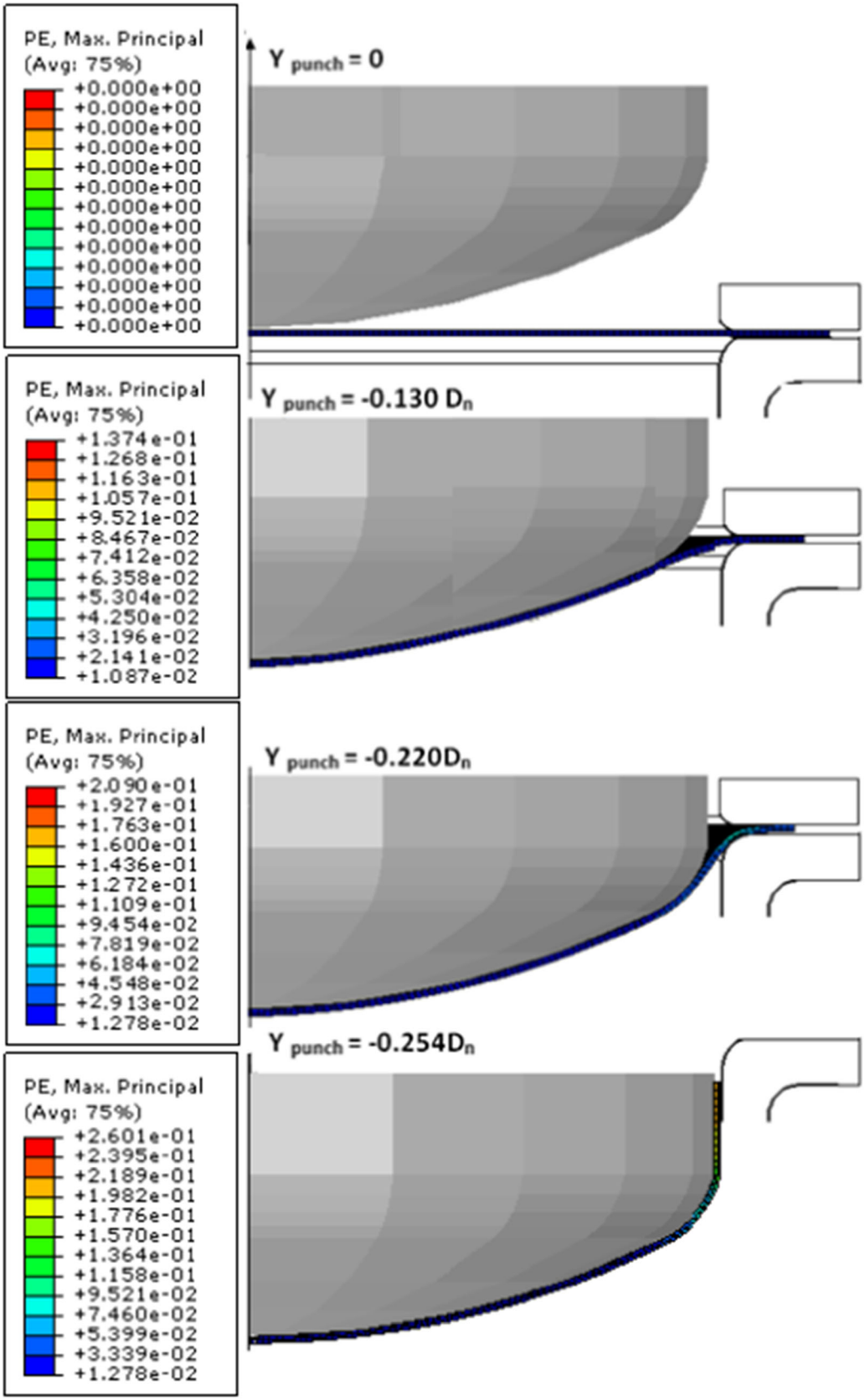


**Fig. 5** PE, Max distribution on the head during the deep drawing. $Y_{\text{punch}}$ is the position of the punch, and it is zero when the die touches the blank

**Table 3** Design simulations for deep drawing of ellipsoidal head air brake pressure reservoir (see Figure 4)

| No. | Blank size radius BR (mm) | Blank thickness $t$ (mm) | Punch radius PR (mm) | Punch nose radius $r_p$ (mm) | Bend radius $r_b$ (mm) | Die radius DR (mm) | Die shoulder radius $r_d$ (mm) | Radial clearance between punch radius and die radius $W_c$ (mm) | Cup height of the first draw $h$ (mm) | Blank holder force BHF (N) | Coefficient of friction $\mu$ (%) |
|---|---|---|---|---|---|---|---|---|---|---|---|
| 1 | 184 | 2 | 148 | *26* | 300 | 150 | 10 | 2 | 80 | 1000 | 0.1 |
| 2 | 184 | 2 | 148 | *28* | 300 | 150 | 10 | 2 | 80 | 1000 | 0.1 |
| 3 | 184 | 2 | 148 | *30* | 300 | 150 | 10 | 2 | 80 | 1000 | 0.1 |
| 4 | 184 | 2 | 148 | *32* | 300 | 150 | 10 | 2 | 80 | 1000 | 0.1 |
| 5 | 184 | 2 | 148 | *34* | 300 | 150 | 10 | 2 | 80 | 1000 | 0.1 |
| 6 | 184 | 2 | 148 | 30 | 300 | 150 | *6* | 2 | 80 | 1000 | 0.1 |
| 7 | 184 | 2 | 148 | 30 | 300 | 150 | *8* | 2 | 80 | 1000 | 0.1 |
| 8 | 184 | 2 | 148 | 30 | 300 | 150 | *10* | 2 | 80 | 1000 | 0.1 |
| 9 | 184 | 2 | 148 | 30 | 300 | 150 | *12* | 2 | 80 | 1000 | 0.1 |
| 10 | 184 | 2 | 148 | 30 | 300 | 150 | *14* | 2 | 80 | 1000 | 0.1 |
| 11 | *184* | 2 | 148 | 30 | 300 | 150 | 10 | 2 | 80 | 1000 | 0.1 |
| 12 | *187* | 2 | 148 | 30 | 300 | 150 | 10 | 2 | 80 | 1000 | 0.1 |
| 13 | *190* | 2 | 148 | 30 | 300 | 150 | 10 | 2 | 80 | 1000 | 0.1 |
| 14 | *193* | 2 | 148 | 30 | 300 | 150 | 10 | 2 | 80 | 1000 | 0.1 |

interesting to know how much extra material within the blank should be permitted in order to avoid defects as far as the overall external dimension such as the external diameter of the head fits within the cylinder of the pressure reservoir.

So starting from the existing procedure, design simulations have been oriented to the effect of overestimating the blank diameter for the configuration of a head part given in Fig. 3d. The next investigation consists in increasing the diameter of the blank by increment of 0.02% of the recommended blank diameter. In this case study, the blank diameter has been increased up to 0.06% as shown in the design simulations numbered from 11 to 14. Results are given in Table 6.

Overestimating the blank diameter does not alter the value of the outer diameter $D_{out}$ of the blank as it is rather dependent on the punch diameter. Meanwhile, the straight flange height $h_1$ and the depth of dishing $h_2$ increase up to deviating from the required standard dimensions of the G.R.C head. The standard deviation is expressed in terms of coefficient of variations given in Table 6 and are plotted in Fig. 6. In fact, the excessive material in the blank is put on the straight flange height $h_1$ and it is the last part to be formed, and a small amount is taken by the depth of dishing $h_2$. However, the effect is better shown on the standard deviation of the total internal head height $H_{int}$ that shows a linear evolution expressed by Eq. (1).

$$Cv_{Hint} = -0.777D + 285.27\% \quad (1)$$

Apart from a slight deviation in the 386 blank diameter, the crown radius $R_i$ and the knuckle radius $r_c$ are not that much affected by the increase of the blank diameter as it can be seen in Fig. 7.

**Table 4** Effect of punch corner radius on the overall dimensions of ellipsoidal head for air brake pressure reservoir (see Figures 3d and 4)

| No. | $r_p$ (mm) | $h_1$ (mm) | $h_2$ (mm) | $H$ (mm) | $D_{ext}$ (Mm) | $R_i$ (Mm) | $r_c$ (mm) | $CV_{h1}$ (%) | $CV_{h2}$ (%) | $CV_{Dext}$ (%) | $CV_{Ri}$ (%) | $CV_{rc}$ (%) |
|---|---|---|---|---|---|---|---|---|---|---|---|---|
| 1 | 26.00 | 20.48 | 54.87 | 75.35 | 300.00 | 296.68 | 26.06 | 0.10 | 2.88 | 0.00 | 1.11 | − 0.23 |
| 2 | 28.00 | 20.53 | 55.94 | 76.47 | 300.00 | 297.44 | 28.61 | − 0.15 | 0.99 | 0.00 | 0.85 | − 2.18 |
| 3 | *30.00* | *20.54* | *56.23* | *76.77* | *300.00* | *300.93* | *30.08* | *− 0.20* | *0.48* | *0.00* | *− 0.31* | *− 0.27* |
| 4 | 32.00 | 20.42 | 56.69 | 77.11 | 300.00 | 299.19 | 32.16 | 0.39 | − 0.34 | 0.00 | 0.27 | − 0.50 |
| 5 | 34.00 | 20.35 | 58.20 | 78.55 | 399.97 | 304.23 | 34.00 | 0.72 | − 3.01 | 0.01 | − 1.41 | − 0.01 |
| Mean value | | 20.46 | 56.39 | 76.85 | 399.99 | 299.69 | 30.18 | | | | | |
| Required value | | 20.50 | 56.50 | 77.00 | 300.00 | 300.00 | 30.00 | | | | | |
| CV (%) | | 0.17 | 0.20 | 0.19 | 0.00 | 0.10 | − 0.61 | | | | | |

**Table 5** Effect of die corner radius on the overall dimensions of ellipsoidal head for air brake pressure reservoir (see Figures 3d and 4)

| No. | $r_d$ (mm) | $h_1$ (mm) | $h_2$ (mm) | $H$ (mm) | $D_{ext}$ (Mm) | $R_i$ (Mm) | $r_c$ (mm) | $CV_{h1}$ (%) | $CV_{h2}$ (%) | $CV_{Dext}$ (%) | $CV_{Ri}$ (%) | $CV_{rc}$ (%) |
|---|---|---|---|---|---|---|---|---|---|---|---|---|
| 6 | 6.00 | 20.64 | 56.61 | 77.25 | 300.00 | 295.09 | 30.65 | − 0.68 | − 0.19 | 0.00 | 1.64 | − 2.17 |
| 7 | 8.00 | 20.53 | 56.41 | 76.94 | 300.00 | 292.73 | 29.87 | − 0.15 | 0.16 | 0.00 | 2.42 | − 2.90 |
| 8 | *10.00* | *20.54* | *56.23* | *76.77* | *300.00* | *300.93* | *30.08* | *− 0.20* | *0.48* | *0.00* | *− 0.31* | *− 027* |
| 9 | 12.00 | 20.39 | 56.86 | 77.25 | 300.00 | 293.34 | 30.35 | 0.54 | − 0.64 | 0.00 | 2.22 | − 1.17 |
| 10 | 14.00 | 20.49 | 56.67 | 77.16 | 300.00 | 306.10 | 30.68 | 0.05 | − 0.30 | 0.00 | − 2.03 | − 2.27 |
| Mean value | | 20.52 | 56.56 | 77.07 | 300.00 | 297.64 | 30.53 | | | | | |
| Required value | | 20.50 | 56.50 | 77.00 | 300.00 | 300.00 | 30.00 | | | | | |
| CV (%) | | − 0.09 | − 0.10 | − 0.10 | 0 | 0.79 | − 1.75 | | | | | |

## 5 Thickness analyses of ellipsoidal heads during drawing process

When drawing thin flat sheet steel into deep-shaped parts, the punch applies force on the flat sheet obliging the material to flow over the die corner radius and then continues straight in the cavity of the die. During the drawing process, changes in steel thickness occur because the material is subjected to tensile stress as illustrated in Fig. 8, showing the plastic elongation and stresses that will obviously cause the dish to thin. Basically, when correctly drawn, some amount of thinning is unavoidable particularly on the knuckle and crown zone where up to 25% reduction of thickness may occur. Therefore, controlling the

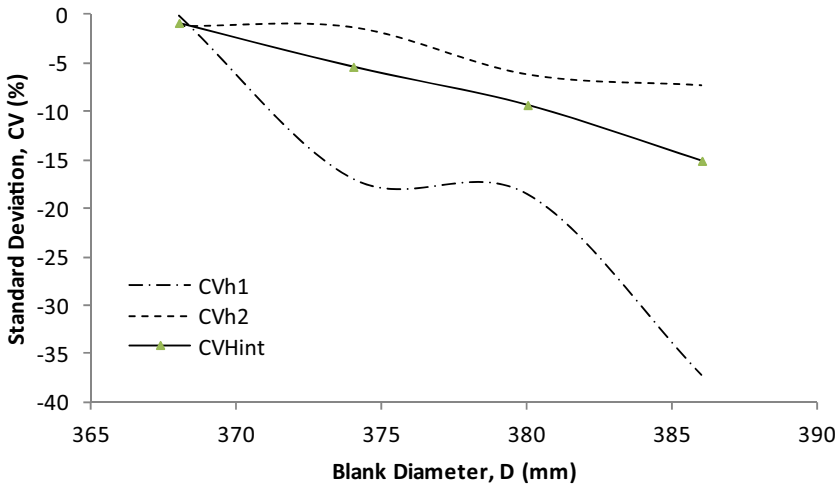


**Fig. 6** Evolution of standard deviation on heights of 300 outer diameter G.R.C heads as a function of blank diameter

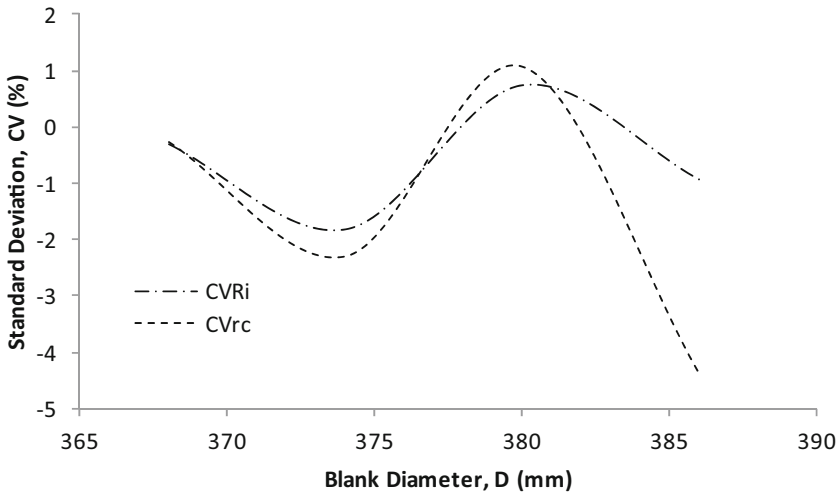


**Fig. 7** Evolution of standard deviation on crown radius and knuckle radius of 300 outer diameter G.R.C heads as a function of blank diameter

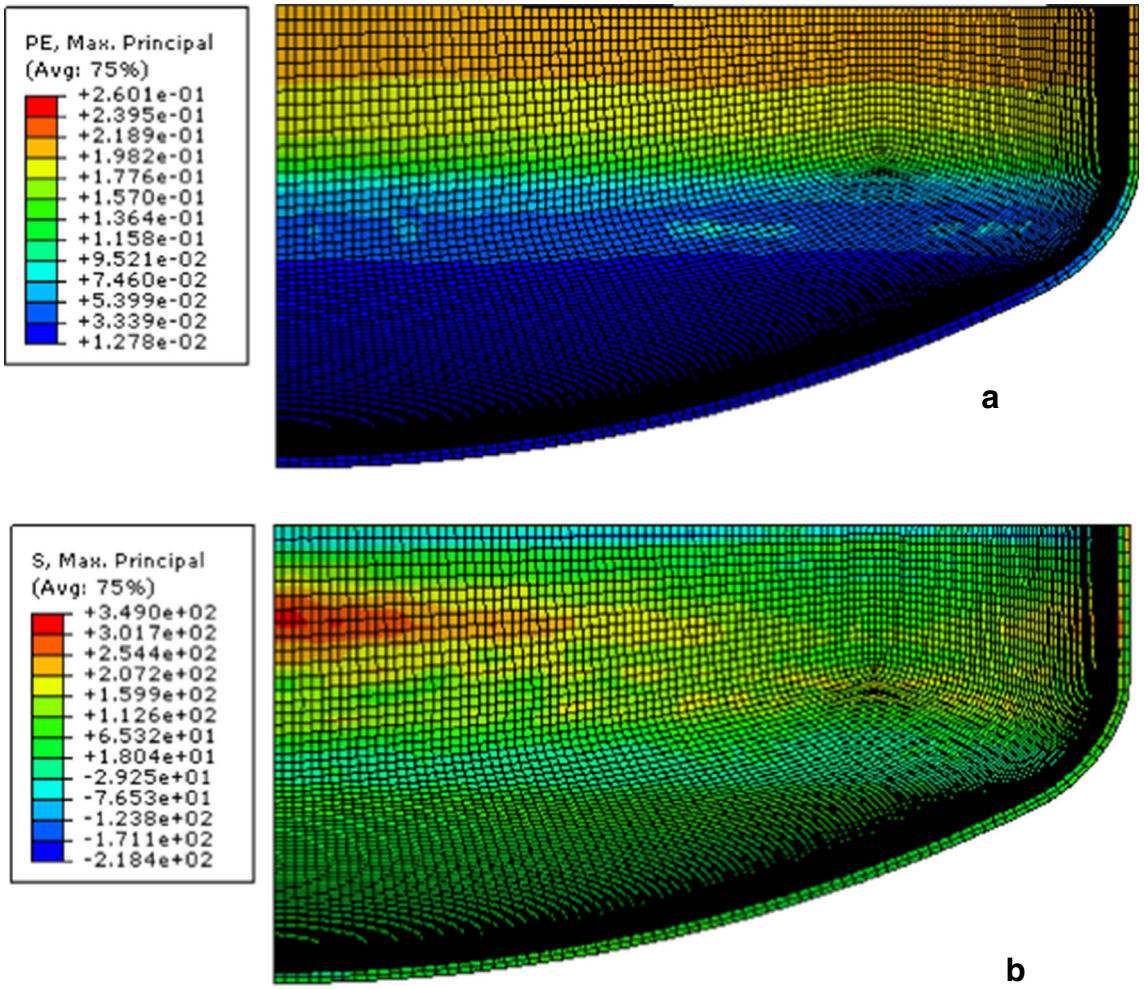


**Fig. 8** Simulation results. **a** Plastic elongation. **b** Stresses

deep drawing process factors in order to mitigate thinning will be of great interest in improving the reliability of air pressure reservoirs. So the next discussions are oriented to the factors controlling the changes in metal thickness when deep drawing the ellipsoidal head of air brake pressure reservoirs. Figure 9 shows the profile characterized by a dish shape showing three zones, the straight flange,

the knuckle, and the crown zones. Along the generated profile, target points have been selected in order to measure the corresponding dish thickness (Table 6).

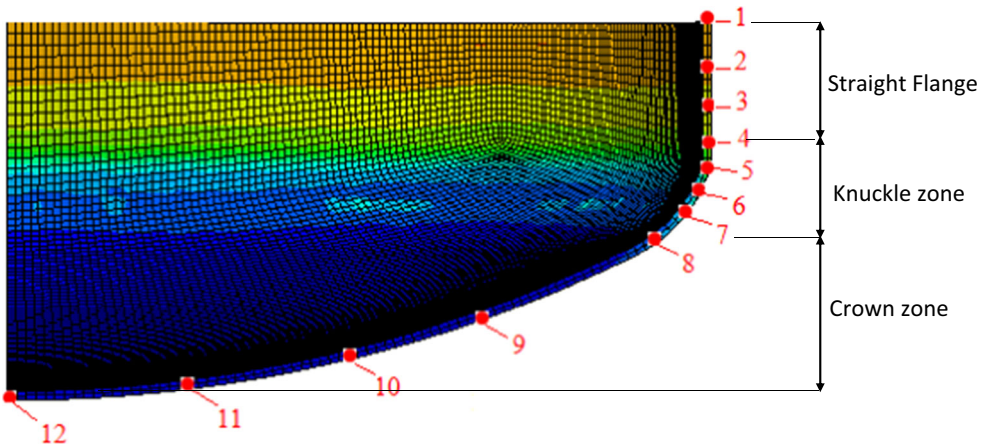


**Fig. 9** Thickness measurement target points

**Table 6** Effect of 6-mm increment in 300-mm blank diameter on the overall dimensions of 300-mm outer diameter of the ellipsoidal head for air brake pressure reservoir (see Figures 3d and 4)

| No. | $D$ (mm) | $h_1$ (mm) | $h_2$ (mm) | $D_{out}$ (Mm) | $R_i$ (Mm) | $r_c$ (mm) | $CV_{h1}$ (%) | $CV_{h2}$ (%) | $CV_{Dext}$ (%) | $CV_{Ri}$ (%) | $CV_{rc}$ (%) | $H_{int}$ (mm) | $CV_{Hint}$ (%) |
|---|---|---|---|---|---|---|---|---|---|---|---|---|---|
| 1 | 368 | 20.54 | 56.23 | 300 | 300.93 | 30.08 | − 0.20 | − 0.12 | 0 | − 0.31 | − 0.27 | 76.77 | − 0.14 |
| 2 | 374 | 23.88 | 57.26 | 300 | 305.42 | 30.69 | − 16.49 | − 1.35 | 0 | − 1.81 | − 2.30 | 81.14 | − 5. |
| 3 | 380 | 24.20 | 59.98 | 300 | 297.81 | 29.68 | − 18.05 | − 6.16 | 0 | 0.73 | 1.07 | 84.18 | − 9.32 |
| 4 | 386 | 28.01 | 60.60 | 300 | 302.80 | 31.31 | − 36.63 | − 7.26 | 0 | − 0. | − 4.37 | 88.61 | − 15.08 |

### 5.1 Evolution of thickness profile as a function of punch corner radius

The variation of the metal thickness in stamped ellipsoidal head when using punches with different corner radius is shown in Fig. 10. As expected, thinning occurs in the three zones and a maximum thinning resulting in plastic strain of 9% of the initial thickness is observed at the border between the straight flange zone and the knuckle zone where the material has been pulled off to fulfill the required shape of the dish. Then, as the crown zone is reached, thinning decreases to about 1.5%. Within the crown zone, thinning follows the curvature of the dish bottom showing a further slight decrease in the center.

### 5.2 Effect of punch radius on true strain along path dish

The best approach to analyze the influence of thinning on the resistance of the dish is to analyze the behavior of the resulted strain where thinning has occurred. Therefore, the thinning profile is plotted in terms of true strain as a function of true distance of the dish for different values of the punch corner radius. As the behavior of the strain in the knuckle zone is different from that in the crown zone, these are presented in two plots (Fig. 11a, b).

In the knuckle zone (Fig. 11a), as the true distance along the path increases, the true strain increases. At the limit of the straight zone and the knuckle zone, using the 30-mm punch nose radius corresponding to the desired radius of the crown zone, no thinning occurred. But when changing the punch nose radius, small thinning occurred and depends on the punch nose radius. Starting from punch nose radius of 26 mm, the true strain was 0.015% then decreases to nearly 0% when $r_p = 34$ mm. As the knuckle-crown zone limit is reached, the true strain increased according to a trend that is best presented by fittings curves in the form of second-order polynomial expressed by Eq. (2).

$$\varepsilon_{kz} = A_{kz}(D_t)^2 + B_{kz}(D_t) + C_{kz} \tag{2}$$

where:

$\varepsilon_{kz}$ is the thickness in the knuckle zone of the ellipsoidal head

$D_t$ is the true distance of the stamped dish in Fig. 10

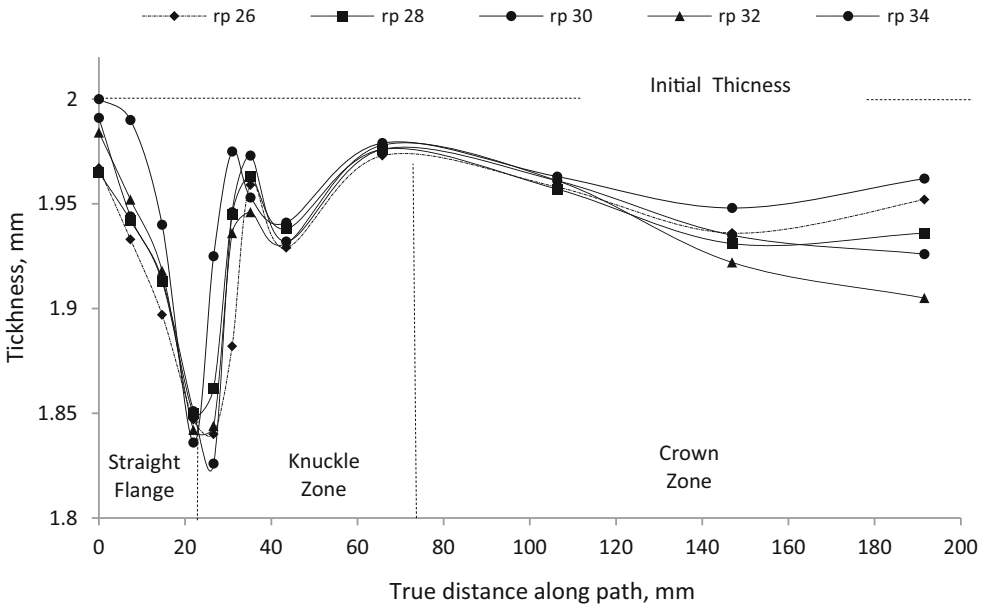


**Fig. 10** Effect of punch corner radius on thickness profile in stamped ellipsoidal head

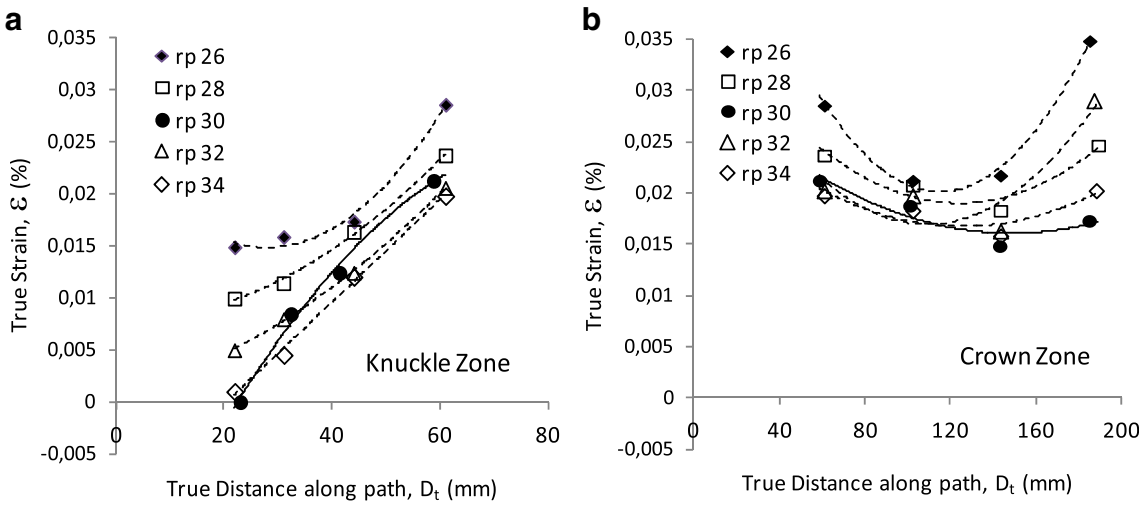


**Fig. 11** Evolution of true strain as a function of true distance along a path of a dish. **a** In the knuckle zone. **b** In the crown zone

$A_{kz}$, $B_{kz}$, and $C_{kz}$ are the two-order polynomial equation parameters given in Table 7

In the crown zone (Fig. 11b), the true strain fitting curves also followed a trend in the form of second-order polynomial model but with different values of the equation parameters. Therefore, the model can be expressed by Eq. (3).

$$\varepsilon_{cz} = A_{cz}(D_t)^2 + B_{cz}(D_t) + C_{cz} \quad (3)$$

where:

$\varepsilon_{cz}$ is the thickness in the crown zone of the ellipsoidal head

$D_t$ is the true distance of the stamped dish in Fig. 10

$A_{cz}$, $B_{cz}$, and $C_{cz}$ are the two-order polynomial equation parameters given in Table 8

The main observation is that for $r_p = 30$ mm, the true strain was law comparing with that obtained when deviating the punch nose radius which corresponds to the knuckle radius $r_c$ of the dish.

**Table 7** Parameters of two-order polynomial equation true strain profile in knuckle zone of ellipsoidal head as a function of punch corner radius

| No. | Punch corner radius | Parameters of two-order polynomial equation of the thickness profile in knuckle zone | | | Coefficient of variation |
|---|---|---|---|---|---|
| | $r_p$ (mm) | $A_{kz}$ | $B_{kz}$ | $C_{kz}$ | $R^2$ |
| 1 | 26 | 0.00001 | − 0.0007 | 0.0248 | 0.9874 |
| 2 | 28 | $4.10^{-6}$ | $-10^{-6}$ | 0.0077 | 0.9975 |
| 3 | 30 | $-7.10^{-6}$ | 0.0011 | 0.0221 | 0.9927 |
| 4 | 32 | $3.10^{-6}$ | − 0.0001 | 0.0009 | 0.9995 |
| 5 | 34 | $-5.10^{-8}$ | − 0.0005 | 0.01 | 0.9963 |

**Table 8** Parameters of two-order polynomial equation true strain profile in crown zone of ellipsoidal head as a function of punch corner radius

| No. | Punch corner radius | Parameters of two-order polynomial equation of the thickness profile in knuckle zone | | | Coefficient of variation |
|---|---|---|---|---|---|
| | $r_p$ (mm) | $A_{cz}$ | $B_{cz}$ | $C_{cz}$ | $R^2$ |
| 1 | 26 | $3.10^{-6}$ | − 0.0007 | 0.0596 | 0.9913 |
| 2 | 28 | $10^{-6}$ | − 0.0003 | 0.0387 | 0.8839 |
| 3 | 30 | $7.10^{-7}$ | 0.0002 | 0.0314 | 0.854 |
| 4 | 32 | $2.10^{-6}$ | − 0.0004 | 0.0391 | 0.8077 |
| 5 | 34 | $8.10^{-7}$ | − 0.0002 | 0.0298 | 0.76 |

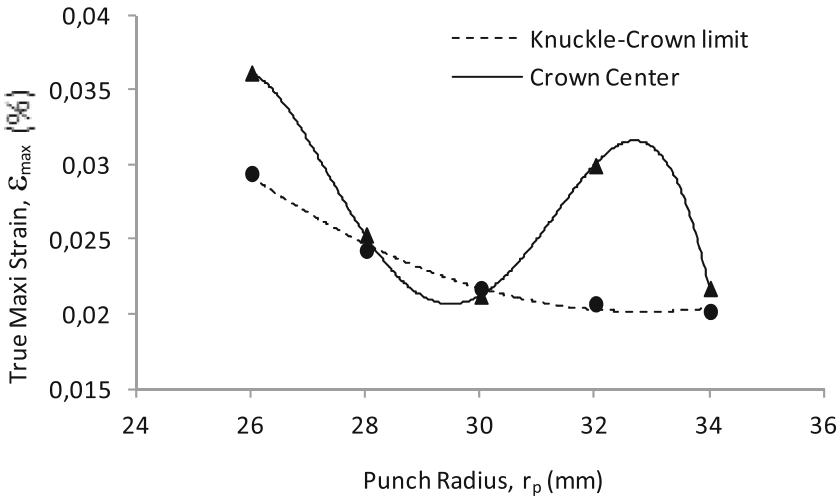


**Fig. 12** Effect of punch radius on maximum true strain

#### 5.2.1 Effect of punch radius on maximum true strain along dish path

The maximum strain as a function of the punch nose radius $r_p$ can be also evaluated through the fitting curves obtained from the plots of maximum strain versus punch radius for values recorded at the knuckle-crown limit and at the crown center (Fig. 12). The latter shows the evolution of maximum true strain recorded at the knuckle-crown zone limit and at the center of the crown zone as a function of punch nose radius $r_p$. This evolution follows a trend that is expressed respectively for strains measured at the knuckle-crown limit by Eq. (4) $\varepsilon_{kzmax}$, which is best fitted by a second polynomial order equation, and for strains recorded at the crown center, $\varepsilon_{czmax}$ is given by a four-order polynomial Eq. (5).

$$\varepsilon_{kzmax} = 0.0002(r_p)^2 - 0.0127(r_p) + 0.2282 \quad (4)$$

$$\varepsilon_{czmax} = -9.10^{-5}(r_p)^4 + 0.0109(r_p)^3 - 0.4796(r_p)^2 + 9.2939 r_p - 67.179 \quad (5)$$

## 6 Conclusion

The present paper proposed a contribution in analyzing dimensional deviations in ellipsoidal thin-layer steel heads of high-pressure reservoir during deep drawing process. The investigation concerned the thinning process occurring while deep drawing to obtain a head according to G.R.C E81-102 standard. Design simulation has followed an industrial case process of deep drawing.

As expected, thinning has occurred in the three zones forming the drawn dish. A maximum thinning is observed at the border between the straight zone and the knuckle zone. The maximum true strain caused by deep drawing approached 9% of the maximum strain of the material. In the crown zone, thinning followed the dish bottom but decreased slightly in its center.

The best performance is observed for the eighth design simulation which is in good agreement with the industrial application.

The behavior of the true strain as a function of punch radius in the knuckle and crown zones is expressed by a respective second-order engineering model. Relatively, the corresponding maximum strain is expressed with a second-order and a four-order degree engineering model.

**Acknowledgements** The authors would like to thank the Algerian truck company SNVI Rouiba for the grateful help and for the furniture of the material. Financial support has been achieved under the research project. Thanks are due to the staff of the metallurgy laboratory of Badji Mokhtar University Annaba for specimen preparation of tensile tests. A great thank to the mechanical laboratory of Alfapipe of the Algerian steel company in El-Hadjar, Annaba, for analyzing the composition of the material.

**Nomenclature** A%, ultimate elongation (%); $E$, Young modulus (GPa); $\sigma_{y0.2}$, yield strength (MPa); $\sigma_{ts}$, tensile strength (MPa)



## References

1. Wasbari F, Bakar RA, Gan LM, Tahir MM, Yusof AA (2017) A review of compressed-air hybrid technology in vehicle system. Renew Sust Energ Rev 67:935–953. https://doi.org/10.1016/j.rser.2016.09.039
2. Petrenko V (2017) Railway rolling stock compressors capacity and main reservoirs volume calculation methods, 10th International Scientific Conference Transbaltica 2017: Transportation Science and Technology. Procedia Eng 187:672–679. https://doi.org/10.1016/j.proeng.2017.04.430
3. Zein H, El Sherbiny M, Abd-Rabou M, El Shazly M (2014) Thinning and spring back prediction of sheet metal in the deep drawing process. Mater Des 53:797–808. https://doi.org/10.1016/j.matdes.2013.07.078
4. Choi J, Choi B, Heo S, Oh Y, Shin S (2018) Numerical modeling of the thermal deformation during stamping process of an automotive body part. Appl Therm Eng 128:159–172. https://doi.org/10.1016/j.appl.therma.leng.2017.09.001

5. Choubey AK, Agnihotri G, Sasikumar C (2017) Experimental and mathematical analysis of simulation results for sheet metal parts in deep drawing. J Mech Sci Technol 31(9):4215–4220. https://doi.org/10.1007/s12206-017-0819-4
6. Dhooge A, Dolby RE, Sebille J, Steinmetz R, Vinckier AG (1978) A review of work related to reheat cracking in nuclear reactor pressure vessel steels. Int J Press Vessel Pip 6(5):329–409. https://doi.org/10.1016/0308-0161(78)90023-6
7. Margolin BZ, Shvetsova VA, Karzov GP (1997) Brittle fracture of nuclear pressure vessel steels - I. Local criterion for cleavage fracture. Int J Press Vessel Pip 72(1):73–87. https://doi.org/10.1016/S0308-0161(97)00012-4
8. Li Y, Chen X, Liu Z, Sun J, Li F, Li J, Zhao G (2017) A review on the recent development of incremental sheet-forming process. Int J Adv Manuf Technol 91:1381–1390. https://doi.org/10.1007/s00170-017-0251-z
9. Takalkar AS, Lenin Babu MC (2018) A review on effect of thinning, wrinkling and spring-back on deep drawing process. Proc IMechE Part B J Eng Manuf IMechE 2018:1–26. https://doi.org/10.1177/0954405417752509
10. Kitayama S, Natsume S, Yamazaki K, Han J, Uchida H (2015) Numerical investigation and optimization of pulsating and variable blank holder force for identification of formability window for deep drawing of cylindrical cup. Int J Adv Manuf Technol 82:583–593. https://doi.org/10.1007/s00170-015-7385-7
11. Kitayama S, Yamada S (2016) Simultaneous optimization of blank shape and variable blank holder force of front side member manufacturing by deep drawing. Int J Adv Manuf Technol 91:1381–1390. https://doi.org/10.1007/s00170-016-9837-0
12. Liu W, An L, Yuan S (2017) Enhancement on deformation uniformity of double curvature shell by hydroforming process and curved blank-holder surface. Int J Adv Manuf Technol 92:1913–1922. https://doi.org/10.1007/s00170-017-0301-6
13. Takalkar AS, Lenin Babu MC, Thampan GK, Rao JMK, Srinivas K (2015) Influence of process parameters on thickness variation of multistage deep drawing process. Indian Conference on Applied Mechanics (INCAM), IIT Delhi, 13–15 July 2015 Page 1 of 6. https://www.researchgate.net/publication/320076017
14. Zheng J, Shu X, Wu Y, Xu H, Lu Q, Liao B, Zhang B (2018) Investigation on the plastic deformation during the stamping of ellipsoidal heads for pressure vessels. Thin-Walled Struct 127:135–144. https://doi.org/10.1016/j.tws.2018.01.040
15. Ghennai W, Boussaid O, Bendjama H, Haddag B, Nouari M (2018) Experimental and numerical study of DC04 sheet metal behaviour—plastic anisotropy identification and application to deep drawing. Int J Adv Manuf Technol. https://doi.org/10.1007/s00170-018-2700-8